Journal of Nuclear Medicine, published on November 2, 2023 as doi:10.2967/jnumed.123.265856

[^{18}F]PI-2620 Binding Patterns in Patients with Suspected Alzheimer Disease and Frontotemporal Lobar Degeneration

Ganna Blazhenets*[1,2], David N. Soleimani-Meigooni*[1], Wesley Thomas[3], Nidhi Mundada[1], Matthias Brendel[4], Stephanie Vento[1], Lawren VandeVrede[1], Hilary W. Heuer[1], Peter Ljubenkov[1], Julio C. Rojas[1,5], Miranda K. Chen[1], Alinda N. Amuiri[1], Zachary Miller[1], Maria L. Gorno-Tempini[1], Bruce L. Miller[1], Howie J. Rosen[1], Irene Litvan[6], Murray Grossman†[7], Brad Boeve[8], Alexander Pantelyat[9], Maria Carmela Tartaglia[10], David J. Irwin[7], Brad C. Dickerson[11], Suzanne L. Baker[3], Adam L. Boxer[1], Gil D. Rabinovici[1,5,12], and Renaud La Joie[1]

[1]Memory and Aging Center, Department of Neurology, University of California, San Francisco, San Francisco, California; [2]Department of Nuclear Medicine, Faculty of Medicine, Medical Center–University of Freiburg, University of Freiburg, Freiburg, Germany; [3]Lawrence Berkeley National Laboratory, Berkeley, California; [4]Department of Nuclear Medicine, University Hospital of Munich, LMU Munich, Munich, Germany; [5]Weill Institute for Neurosciences, University of California, San Francisco, San Francisco, California; [6]University of California, San Diego, San Diego, California; [7]Penn FTD Center, University of Pennsylvania, Philadelphia, Pennsylvania; [8]Mayo Clinic, Rochester, Minnesota; [9]Johns Hopkins University School of Medicine, Baltimore, Maryland; [10]University of Toronto, Toronto, Ontario, Canada; [11]Massachussets General Hospital, Boston, Massachusetts; and [12]Department of Radiology and Biomedical Imaging, University of California, San Francisco, San Francisco, California

Tau PET has enabled the visualization of paired helical filaments of 3 or 4 C-terminal repeat tau in Alzheimer disease (AD), but its ability to detect aggregated tau in frontotemporal lobar degeneration (FTLD) spectrum disorders is uncertain. We investigated 2-(2-([^{18}F]fluoro)-pyridin-4-yl)-9*H*-pyrrolo[2,3-b:4,5c′]dipyridine ([^{18}F]PI-2620), a newer tracer with ex vivo evidence for binding to FTLD tau, in a convenience sample of patients with suspected FTLD and AD using a static acquisition protocol and parametric SUV ratio (SUVr) images. **Methods:** We analyzed [^{18}F]PI-2620 PET data from 65 patients with clinical diagnoses associated with AD or FTLD neuropathology; most (60/65) also had amyloid-β (Aβ) PET. Scans were acquired 30–60 min after injection; SUVr maps (reference, inferior cerebellar cortex) were created for the full acquisition and for 10-min truncated sliding windows (30–40, 35–45, … 50–60 min). Age- and sex-adjusted *z* score maps were computed for each patient, relative to 23 Aβ-negative cognitively healthy controls (HC). Mean SUVr in the globus pallidus, substantia nigra, subthalamic nuclei, dentate nuclei, white matter, and temporal gray matter was extracted for the full and truncated windows. **Results:** Patients with suspected AD neuropathology (Aβ-positive patients with mild cognitive impairment or AD dementia) showed high-intensity temporoparietal cortex–predominant [^{18}F]PI-2620 binding. At the group level, patients with clinical diagnoses associated with FTLD (progressive supranuclear palsy with Richardson syndrome [PSP Richardson syndrome], corticobasal syndrome, and nonfluent-variant primary progressive aphasia) exhibited higher globus pallidus SUVr than did HCs; pallidal retention was highest in the PSP Richardson syndrome group, in whom SUVr was correlated with symptom severity ($\rho = 0.53$, $P = 0.05$). At the individual level, only half of PSP Richardson syndrome, corticobasal syndrome, and nonfluent-variant primary progressive aphasia patients had a pallidal SUVr above that of HCs. Temporal SUVr discriminated AD patients from HCs with high accuracy (area under the receiver operating characteristic curve, 0.94 [95% CI, 0.83–1.00]) for all time windows, whereas discrimination between patients with PSP Richardson syndrome and HCs using pallidal SUVr was fair regardless of time window (area under the receiver operating characteristic curve, 0.77 [95% CI, 0.61–0.92] at 30–40 min vs. 0.81 [95% CI, 0.66–0.96] at 50–60 min; $P = 0.67$). **Conclusion:** [^{18}F]PI-2620 SUVr shows an intense and consistent signal in AD but lower-intensity, heterogeneous, and rapidly decreasing binding in patients with suspected FTLD. Further work is needed to delineate the substrate of [^{18}F]PI-2620 binding and the usefulness of [^{18}F]PI2620 SUVr quantification outside the AD continuum.

Key Words: FTLD; PI2620; tau PET; Alzheimer disease

J Nucl Med 2023; 00:1–10
DOI: 10.2967/jnumed.123.265856

Tau is a microtubule-associated protein that is present in 6 different isoforms through alternative splicing of messenger RNA of exons 2, 3, and 10. Inclusion of exon 10 results in the production of 3 isoforms with 4 C-terminal repeats (4R), and its exclusion results in another 3 isoforms with 3 repeats (3R). Most of the currently available tau PET radioligands were designed to detect Alzheimer disease (AD) pathology, that is, mixed 3- and 4-repeat (3R/4R) tau aggregated in paired helical filaments (*1,2*). In contrast, frontotemporal lobar degeneration (FTLD) is a heterogeneous spectrum of neurodegenerative disorders that are subclassified into 3 major neuropathologic categories based on the specific protein inclusions: FTLD tau, FTLD TAR DNA-binding protein 43 (TDP-43), and FTLD fused in sarcoma (*3*). Unlike AD, FTLD tau includes various tauopathies that are characterized by neuronal or glial aggregates of either 3R or 4R tau (*4,5*). For example, progressive supranuclear palsy (PSP) and corticobasal degeneration are 2 primary FTLD tauopathies, as are most familial cases of FTLD tau due to mutations in the tau gene *MAPT*. Molecular imaging of FTLD primary tauopathies (e.g., with [^{18}F]flortaucipir PET) has been challenging because of a lower density of tau aggregates in these disorders than in AD.

2-(2-([^{18}F]fluoro)pyridin-4-yl)-9*H*-pyrrolo[2,3-b:4,5c′]dipyridine ([^{18}F]PI-2620) tau PET may have potential to overcome some of

Received Apr. 13, 2023; revision accepted Sep. 27, 2023.
For correspondence or reprints, contact Renaud La Joie (renaud.lajoie@ucsf.edu).
*Contributed equally to this work.
†Deceased.
Published online Nov. 2, 2023.

these limitations. Preclinical evaluations found that [^{18}F]PI-2620 lacked off-target binding to monoamine oxidases (*6*) and had high-affinity binding to both mixed 3R/4R and 4R tau, with the −log10 of the half-maximal inhibitory concentration being 8.5 (*6*) and 11.1 (*7*) in AD, 11.3 in corticobasal degeneration (*7*), and 7.7 (*6*) and 8.6 (*7*) in PSP brain tissue. [^{18}F]PI-2620 has been able to detect tau aggregates in patients with a clinical diagnosis of AD (*2,8*) and syndromes associated with a greater probability of underlying FTLD tau pathology, including PSP (*9*) and corticobasal syndrome (CBS) (*10*). Moreover, [^{18}F]PI-2620 has been granted orphan drug designation as a diagnostic tool for PSP and corticobasal degeneration by both the European Commission and the U.S. Food and Drug Administration.

In this exploratory observational study, we aimed to characterize [^{18}F]PI-2620 binding among different clinical syndromes associated with AD versus FTLD pathology. According to the clinical need to have a simplified quantification routine with SUV ratio (SUVr) and shorter acquisition protocols, we explored 30 to 60 min after injection as a possible acquisition window, instead of the full dynamic evaluation, for patients with suspected AD and FTLD pathologies. This window was selected among available acquired data as closest to a previously suggested 20- to 40-min acquisition (*11*). Additionally, this study aimed to analyze sliding 10-min time windows to inspect SUVr behavior over time in each diagnostic group.

MATERIALS AND METHODS

Cohort and Clinical Assessments

This cross-sectional observational study enrolled participants from a large outpatient pool who underwent tau PET with [^{18}F]PI-2620. This convenience sample included 35 consecutive participants enrolled in the multicenter 4 Repeat Tauopathy Neuroimaging Initiative–Cycle 2 (4RTNI-2; U.S. National Institutes of Health grant 2R01AG038791-06A1) cohort and 30 consecutive participants enrolled in the University of California, San Francisco, Alzheimer's Disease Research Center (U.S. National Institute on Aging grant P30-AG062422), as of December 15, 2022. All participants gave their medical history and underwent a neurologic examination, genetic testing, cognitive testing (Mini-Mental State Examination), functional rating assessments (PSP rating scale (*12*), clinical dementia rating (*13*), clinical dementia rating dementia staging instrument plus National Alzheimer's Coordinating Center behavior and language domains (*14*)), and brain MRI following study-specific protocols. All but 5 participants also underwent [^{18}F]florbetapir (4RTNI-2) or [^{18}F]florbetaben PET to evaluate for the presence of brain amyloid-β (Aβ) neuropathology.

Aβ-positive patients with clinically diagnosed amnestic and nonamnestic mild cognitive impairment (MCI) due to AD or AD dementia (ADD) were combined into an Aβ-positive MCI/ADD group (*15*). This included 3 patients with logopenic-variant primary progressive aphasia (PPA) and one patient with posterior cortical atrophy, both of which are atypical clinical variants of AD (*16,17*). Aβ-negative cognitively impaired individuals (MCI or dementia) were suspected to have non-AD pathology and were assigned to the Aβ-negative MCI or dementia group. Clinical diagnoses for patients with suspected FTLD pathology were made by consensus application of standard research criteria (*16,18,19*). PSP with Richardson syndrome (PSP Richardson syndrome) and CBS are the clinical syndromes most associated with FTLD tau. Previous data on 25 nonfluent-variant PPA participants from our center determined that this syndrome was also associated with FTLD tau in 88% of cases (*20*). Participants who met the clinical criteria (*16,21*) for behavioral-variant frontotemporal dementia were suspected to have either FTLD tau or FTLD TDP-43 pathology, and participants with a clinical diagnosis of semantic-variant PPA were suspected to have FTLD TDP-43 pathology (*20*). Participants with behavioral-variant frontotemporal dementia and semantic-variant PPA were evaluated separately from participants with PSP Richardson syndrome, CBS, and nonfluent-variant PPA. Cognitively unimpaired Aβ-negative healthy controls (HCs) from 4RTNI-2 (n = 3); the University of California, San Francisco, Alzheimer's Disease Research Center (n = 8); and Brendel et al. (*9*) (n = 12) were used as controls.

Local institutional review boards approved the study. Written informed consent was obtained from all participants or designated decision-makers before protocol-specific procedures were performed.

PET Data Acquisition, Processing, and Harmonization

[^{18}F]PI-2620 PET data were acquired at multiple sites and various acquisition windows (Supplemental Table 1; supplemental materials are available at http://jnm.snmjournals.org), all of which included 30–60 min after tracer injection reconstructed as 5-min frames. Inferior cerebellar gray matter (supplemental discussion (*2,22–26*)) was defined by segmentation and parcellation of each individual's MR images (FreeSurfer, version 7; https://surfer.nmr.mgh.harvard.edu/) and the spatially unbiased infratentorial toolbox cerebellar template (*27*) and was used as the reference region during calculation of SUVr for the full acquisition (30 min) and the 10-min truncated windows (30–40, 35–45, 40–50, 45–55, and 50–60 min) (*11*). SUVr maps were warped to Montreal Neurological Institute space for voxelwise analyses using statistical parametric mapping software (SPM12; Wellcome Center for Human Neuroimaging). Group-averaged [^{18}F]PI-2620 SUVr maps were created for qualitative assessment of the global pattern of tracer retention in groups with at least 5 patients. Details on PET data processing are in the supplemental methods (*28–30*).

Group-Level Analysis of PET Data

Statistical analyses were performed using R. Demographic, clinical, and cognitive variables were compared by ANOVA or χ^2 testing of independence. Associations between [^{18}F]PI-2620 SUVr and age, cognitive testing scores, or other imaging biomarkers were measured by Spearman correlation (ρ).

Exploratory voxelwise comparisons were performed between each patient group and HCs by analysis of covariance, controlling for the subject's age and sex, in SPM12. Given the small sample size of some groups, an uncorrected P value of less than 0.01 (cluster extent of at least 100 isotropic voxels, ∼0.33 mL) was chosen as a significance threshold. Because it may be recommended to use nonparametric statistics with small sample sizes, we repeated analysis of covariance with statistical nonparametric mapping (SnPM13; University of Warwick) with 5,000 permutations to validate our results.

Mean [^{18}F]PI-2620 SUVr values from multiple regions were extracted in native space (Supplemental Fig. 1). Regions with the highest expected tau burden in each group were selected on the basis of the known distribution of tau pathology in FTLD and AD described in the neuropathology and neuroimaging literature (*1,9,31*). To quantify AD-associated tau PET signal, a temporal meta–region of interest (meta-ROI) SUVr was computed on the basis of FreeSurfer segmentation (*32*). To detect FTLD-associated tau PET signal, the globus pallidus (lateral and medial combined), substantia nigra, dentate nuclei, and subthalamic nuclei ROIs from the atlas of Ilinsky et al. (*33*) were reverse-normalized from Montreal Neurological Institute space to each patient's native space, and SUVr values in each region were extracted. Cerebral white matter (WM) was defined by FreeSurfer segmentation and eroded multiple times to preserve only the centrum semiovale and minimize the impact of spillover from the cortex in patients with high cortical uptake. The positioning of all ROIs was visually quality-controlled by overlaying them on the individual's anatomic MR images. Extracted mean SUVr values were compared between groups by ANOVA (adjusted for age and sex) followed by the Tukey honestly-significant-difference test. Effect size was estimated by Cohen d. Finally, we tested the intergroup differences in

SUVr for the 10-min truncated sliding-acquisition windows using repeated-measures ANOVA, with the time window being the within-subject factor and group being the between-subject factor.

Receiver operating characteristic analysis was performed to test the ability of selected regions to differentiate patients from HCs for the full and truncated windows. Bootstrap resampling (nonparametric stratified, $n = 2{,}000$) (*34*) was used to determine whether differences in area under the receiver operating characteristic curve (AUC) were significant. Clinical groups with fewer than 5 patients were excluded from statistical comparisons because of limited power and were described at the individual level on the basis of the SUVr and *W*-maps. *W*-maps express deviation of signal from the control group, accounting for age and sex differences.

Data Availability

Data are provided on reasonable request and on approval of the institutional review board. Requests for data from the University of California, San Francisco, Alzheimer's Disease Research Center can be submitted for review and fulfillment online (https://memory.ucsf.edu/research-trials/professional/open-science). 4RTNI data can be requested online from the Laboratory of Neuroimaging Image and Data Archive (https://ida.loni.usc.edu).

RESULTS

Participants and Clinical Diagnoses

Participant characteristics across diagnostic groups are presented in Table 1. Sixty-five patients and 23 HCs were included for analysis. Sixteen patients with MCI or dementia were Aβ-positive on PET and classified as Aβ-positive MCI/ADD. The remaining 5 participants who fulfilled the clinical criteria for MCI or dementia due to AD were Aβ-negative on PET and assigned to the Aβ-negative MCI/D group. Of 16 patients who met the diagnostic criteria for PSP, 14 had PSP Richardson syndrome and 2 had PSP parkinsonism. Eleven patients had a clinical diagnosis of CBS. Twelve participants met the clinical criteria for nonfluent-variant PPA. Behavioral-variant frontotemporal dementia was diagnosed in 3 participants. Two patients met the clinical criteria for semantic-variant PPA. Because of small sample sizes, patients with PSP parkinsonism, behavioral-variant frontotemporal dementia, and semantic-variant PPA were not analyzed as separate groups; we described only individual [^{18}F]PI-2620 PET scans and considered these data points in analyses that included all participants.

Age, sex, age at onset, and disease duration were not significantly different between groups. Aβ-positive MCI/ADD patients had the worst performance on the Mini-Mental State Examination, which differed significantly from HCs ($P < 0.001$). PSP Richardson syndrome patients scored highest on the PSP rating scale ($P < 0.01$). Clinical dementia rating, clinical dementia rating sum of boxes, and clinical dementia rating plus National Alzheimer's Coordinating Center FTLD sum of boxes were significantly increased in the Aβ-positive MCI/ADD group ($P < 0.001$, $P = 0.003$, and $P = 0.002$, respectively) and in the PSP Richardson syndrome group ($P < 0.001$, $P = 0.018$, and $P = 0.013$, respectively). Clinical dementia rating scores were also increased in the nonfluent-variant PPA group ($P = 0.004$).

TABLE 1
Demographic and Clinical Characteristics of Analyzed Cohort

Parameter	Aβ-negative HC	PSP Richardson syndrome	CBS	Nonfluent-variant PPA	Aβ-positive MCI/ADD	Aβ-negative MCI or dementia
Demographic						
n	23	14	11	12	16	5
Age at PET (y)	69 (11)	70 (7)	66 (7)	72 (7)	73 (9)	69 (5)
Male (%)	39	79	26	58	63	40
Age at onset (y)	—	65 (7)	61 (8)	65 (5)	67 (9)	63 (6)
Disease duration (y)	—	5 (4)	5 (3)	5 (3)	5 (2)	4 (3)
Aβ PET (*n*)						
Positive	0	3	3	2	16	0
Available	23	13	8	11	16	5
Clinical testing score						
PSP rating scale	3 (3)	31 (13)*	23 (15)	12 (11)	0 (0)	2 (1)
Clinical dementia rating	0.0 (0.0)	0.9 (0.6)†	0.4 (0.4)	0.6 (0.4)‡	1.0 (0.7)†	0.5 (0.0)
Clinical dementia rating sum of boxes	0 (0)	4 (3)*	3 (3)	3 (3)	5 (4)‡	3 (2)
Clinical dementia rating plus NACC FTLD sum of boxes	0 (0.2)	5 (4)*	3 (3)	5 (3)	6 (5)‡	3 (2)
Mini-Mental State Examination	29 (1)	24 (3)	24 (6)	23 (4)*	20 (8)†	26 (4)

*$P < 0.5$ compared with HC.
†$P < 0.001$ compared with HC.
‡$P < 0.01$ compared with HC.
NACC = National Alzheimer's Coordinating Center.
Qualitative data are number or percentage; continuous data are mean followed by SD. Table does not include 2 patients with semantic-variant PPA, 3 patients with behavioral-variant frontotemporal dementia, and 2 patients with PSP parkinsonism.

Binding at Single-Subject Level

HC. No HC participants had high cortical [^{18}F]PI-2620 binding. WM and off-target signal varied across participants (Fig. 1A). Low tracer binding was noted in the basal ganglia, ventral midbrain, and choroid plexus. The 4 eldest controls (age range, 78–85 y) had mild globus pallidus binding.

AD. Patients in the Aβ-positive MCI/ADD group had a high [^{18}F]PI-2620 SUVr in the temporoparietal cortex, with some patients also showing high occipital and frontal binding (Fig. 1C). Heterogeneity in intensity and asymmetry are explained by disease severity and the presence of patients with logopenic-variant PPA (63, 75, and 81 y old) and posterior cortical atrophy (76 y old) (Supplemental Fig. 2). One Aβ-positive MCI participant (63-y-old man), who was a known *PSEN1* mutation carrier, did not have significant [^{18}F]PI-2620 binding (supplemental discussion and Supplemental Fig. 3). Another Aβ-positive MCI participant (78-y-old man) had mild temporal cortical uptake and high binding in the globus pallidus that was significantly greater than in age- and sex-matched HCs on the *W*-map.

PSP Richardson Syndrome, CBS, Nonfluent-Variant PPA. The intensity of tracer binding in the basal ganglia varied across patients with suspected FTLD, possibly reflecting their etiologic heterogeneity (Fig. 1B). The PSP Richardson syndrome group contained the most patients with elevated uptake in the basal ganglia. Two of 3 Aβ-positive PSP Richardson syndrome patients showed elevated uptake in the basal ganglia, similarly to the rest of the PSP Richardson syndrome group. In both patients with PSP parkinsonism, tracer binding intensity was not different from controls (Supplemental Fig. 4). Considering the heterogeneity of pathologies underlying CBS (*35*), the group was further split into CBS and CBS AD. Three patients with prominent AD-typical cortical binding were grouped into the CBS AD group, whereas the other 8 patients were suspected to have FTLD (Supplemental Fig. 5). Two of 3 CBS AD patients had Aβ PET and were positive on the visual read and on quantification (centiloid units > 24 (*36*)). Four patients with CBS (64, 65, 73, and 75 y old) and 2 patients with nonfluent-variant PPA (60 and 77 y old) had high basal ganglia uptake. The *W*-maps of these 6 patients, when

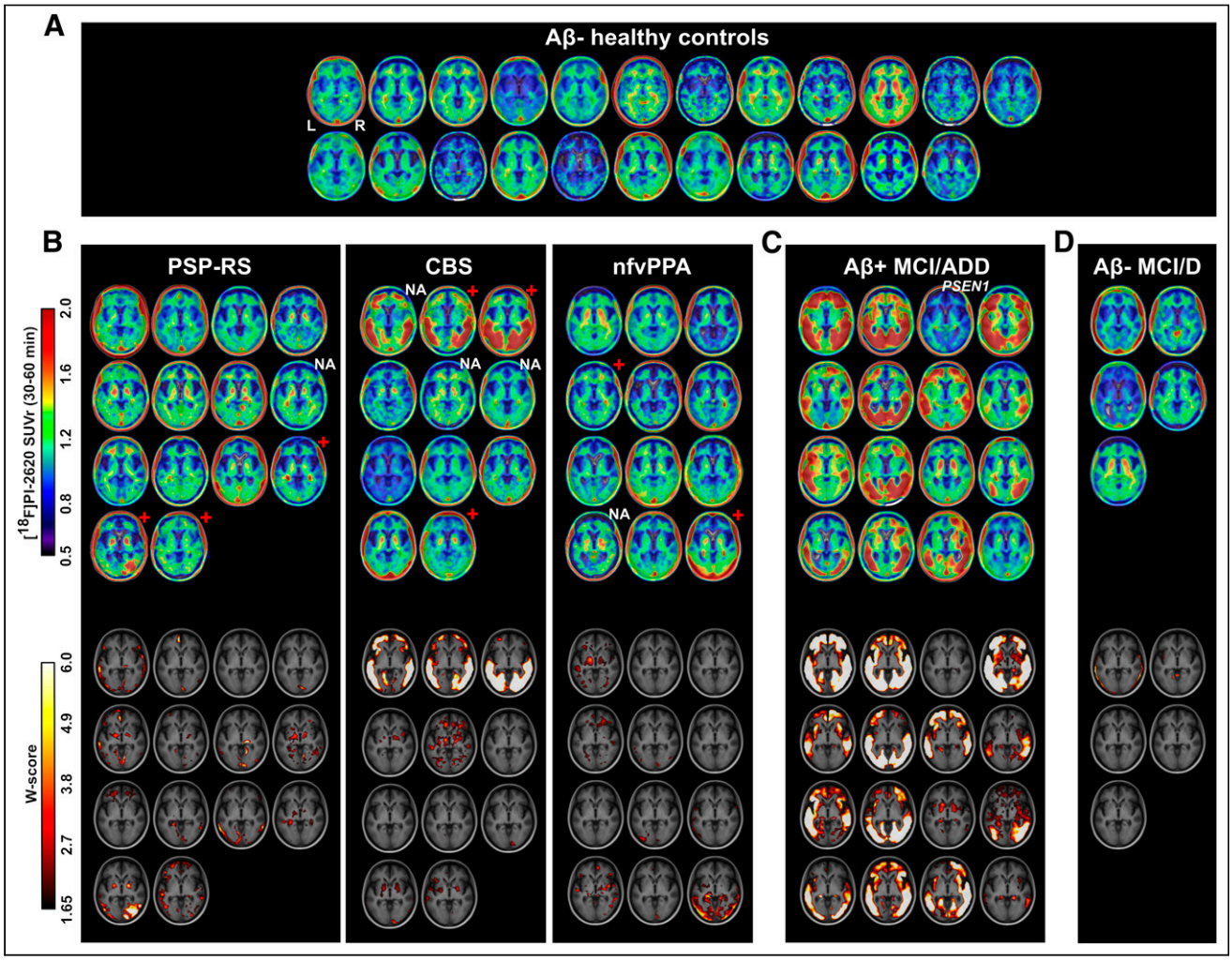

FIGURE 1. Axial slices at level of globus pallidus showing individual [^{18}F]PI-2620 SUVr for controls (A) and suspected FTLD (B), AD (C), and other (D) participants. Each image represents one participant, sorted according to age, within corresponding diagnostic group. Age and centiloid values of presented patients are shown in Supplemental Figure 7. *W*-maps expressing deviation of signal from control group, accounting for age and sex differences, are presented below corresponding SUVr maps. Red cross and NA indicate Aβ-positive or unavailable Aβ PET status for FTLD patients, respectively. *PSEN1* indicates patient with known presenilin-1 gene mutation. D = dementia; nfv = nonfluent variant; RS = Richardson syndrome.

compared with controls, showed high pallidal uptake greater than expected for participant age and sex.

Other. One semantic-variant PPA patient (74-y-old man) was Aβ-positive on PET and showed [^{18}F]PI-2620 cortical binding in a typical AD pattern, strongly suggesting underlying AD pathology. In contrast, the second patient (81-y-old woman) presented with strong bilateral, asymmetric atrophy of the temporal poles, Aβ-positive PET, and very mild [^{18}F]PI-2620 binding in the temporal WM (Fig. 2; Supplemental Fig. 6). Patients with clinical diagnoses of behavioral-variant frontotemporal dementia showed no cortical binding. A behavioral-variant frontotemporal dementia patient with progranulin (*GRN*) mutation showed significantly elevated [^{18}F]PI-2620 binding in the globus pallidus. No tracer binding was observed in the frontal gray matter or WM, where atrophy was the most pronounced. Aβ-negative MCI/D patients had low cortical binding and varying levels of WM and off-target binding. A high SUVr in the pallidum and thalamus was observed in the oldest participant (73-y-old woman); however, this binding was not greater than in HCs according to the *W*-map.

Group Patterns of [^{18}F]PI-2620 Binding

Group-averaged [^{18}F]PI-2620 30- to 60-min SUVr maps are shown in Figure 3. In HC, we observed little to no cortical binding, mild WM off-target binding, and strong off-target binding in the ventral midbrain and extracerebral space (scalp, eye muscles). The Aβ-positive MCI/ADD group had intense, widespread temporoparietal and dorsal frontal cortical binding that was significantly different from that of HCs (familywise error–corrected $P < 0.05$, voxel level). The PSP Richardson syndrome group had significantly higher uptake in the basal ganglia, especially in the globus pallidus, than that of HCs based on visual evaluation and voxelwise analysis (uncorrected $P < 0.01$, Supplemental Fig. 8 shows statistical nonparametric mapping results). In other groups (CBS, nonfluent-variant PPA, and Aβ-negative MCI/D), uptake did not exceed that of HCs in either the cortical regions or the basal ganglia.

Regional Analysis

[^{18}F]PI-2620 SUVr in the eroded WM, dentate nuclei, substantia nigra, and subthalamic nuclei was not different between groups (all $P > 0.1$). Significant group effects were observed for the globus pallidus ($F_{(5,72)} = 2.4$, $P = 0.04$) and temporal meta-ROI ($F_{(5,72)} = 24.7$; $P < 0.001$) (Fig. 4). A group difference in pallidal binding was driven by PSP Richardson syndrome ($d = 1.02$, post hoc $P = 0.02$ compared with HC). Temporal meta-ROI binding was increased only in the Aβ-positive MCI/ADD group ($d = 2.36$, post hoc $P < 0.001$).

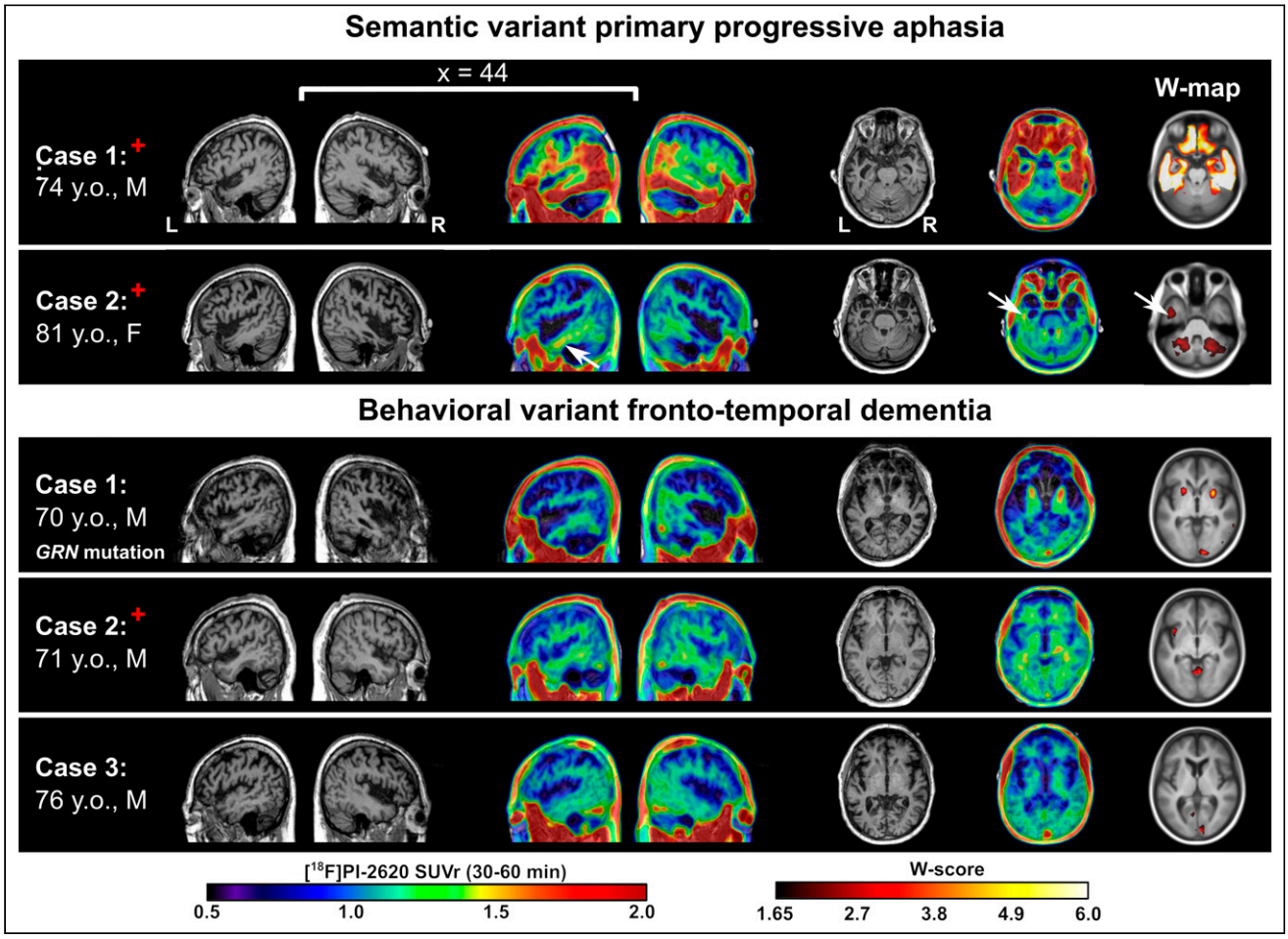

FIGURE 2. Selected sagittal and axial slices of anatomic MRI and [^{18}F]PI-2620 SUVr and *W*-map overlaid on MRI template for participants with semantic-variant PPA and behavioral-variant frontotemporal dementia. White arrows in semantic-variant PPA patient 2 point to mild tracer retention in left temporal WM. Behavioral-variant frontotemporal dementia patient 1 was symptomatic *GRN* mutation carrier. Red cross indicates participants with Aβ-positive PET status.

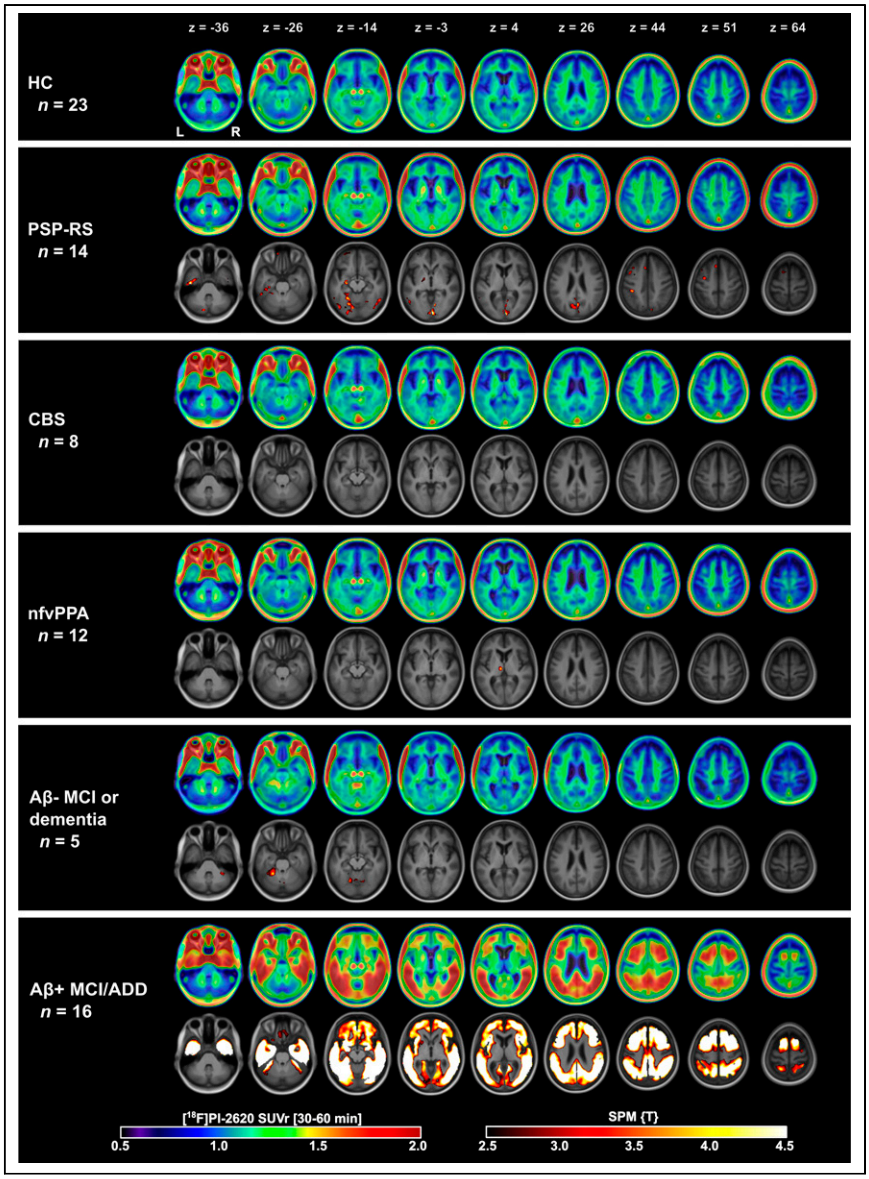

FIGURE 3. Axial slices of group-averaged [^{18}F]PI-2620 SUVr (30–60 min) maps for control and patient groups. For patient groups, second row shows results of voxelwise comparison to control group overlayed on MRI template in Montreal Neurological Institute space. nfv = nonfluent variant; RS = Richardson syndrome; z = slice position in mm.

The other 2 participants with elevated meta-ROI binding were identified to be Aβ-positive FTLD participants, who did not show the typical AD-like cortical pattern (Supplemental Fig. 9). Mean regional SUVr values for each diagnostic group are described in Supplemental Table 2.

In the whole cohort, Aβ PET centiloid unit levels were associated with [^{18}F]PI-2620 SUVr in the temporal meta-ROI ($\rho = 0.66$, $P < 0.001$) but not in the globus pallidus ($\rho = 0.16$, $P = 0.18$) (Fig. 5). On the basis of the observed group differences in the temporal meta-ROI (driven by patients with AD) and in the globus pallidus (driven by patients with PSP Richardson syndrome), these 2 regions were tested for discrimination ability in receiver operating characteristic AUC analysis. The mean SUVr in the temporal meta-ROI allowed for excellent discrimination of the Aβ-positive MCI/ADD group from HCs, with an AUC of 0.94 (95% CI, 0.83–1.00). For PSP Richardson syndrome, the mean SUVr in the globus pallidus allowed for fair discrimination from HCs, with an AUC of 0.80 (95% CI, 0.66–0.94) (Fig. 5B).

Across all groups, basal ganglia and WM SUVr values decreased over time, whereas tracer retention in extracerebral areas (eye muscles, venous sinuses) increased. Receiver operating characteristic AUC analysis showed no difference in AUCs for different time windows (supplemental results and Supplemental Fig. 10).

Associations with Demographic and Clinical Data

There was no significant association between globus pallidus SUVr and age for PSP Richardson syndrome or HC participants ($\rho = 0.13$, $P = 0.64$, and $\rho = 0.24$, $P = 0.25$, respectively) (Fig. 6A). The association between SUVr in temporal meta-ROI and age was not significant for the whole Aβ-positive MCI/ADD group ($\rho = -0.33$, $P = 0.20$), but there was a nonsignificant trend for an association after excluding the patient with *PSEN1* mutation ($\rho = -0.49$, $P = 0.06$). We also observed no association between mean SUVr in eroded WM and age for PSP Richardson syndrome or HC participants (all $P > 0.1$). Voxelwise regression analysis in HCs indicated a positive association between age and SUVr in the putamen but not in the globus pallidus (Supplemental Fig. 12).

In the PSP Richardson syndrome group, the mean SUVr in the globus pallidus was correlated to the total PSP rating scale score ($\rho = 0.53$, $P = 0.05$) (Fig. 6B). Similarly, in the Aβ-positive MCI/ADD group, there was a strong association between SUVr in the temporal meta-ROI and Mini-Mental State Examination scores ($\rho = -0.78$, $P < 0.001$). No significant association between volume and SUVr in the globus pallidus was found for HCs ($\rho = -0.02$, $P = 0.92$) or the Aβ-positive MCI/ADD group ($\rho = 0.17$, $P = 0.51$), and a trend-level association was found for the PSP Richardson syndrome group ($\rho = 0.52$, $P = 0.06$).

DISCUSSION

This exploratory observational study described patterns of [^{18}F]PI-2620 tau PET in a range of neurodegenerative conditions featuring tau pathology. We found intense and consistent [^{18}F]PI-2620 cortical binding in Aβ-positive MCI/ADD patients but lower-intensity, heterogeneous, and rapidly decreasing subcortical binding in patients with PSP Richardson syndrome, CBS, and nonfluent-variant PPA.

In patients with suspected AD neuropathology (Aβ-positive MCI/ADD), [^{18}F]PI-2620 binding was strongly elevated in the

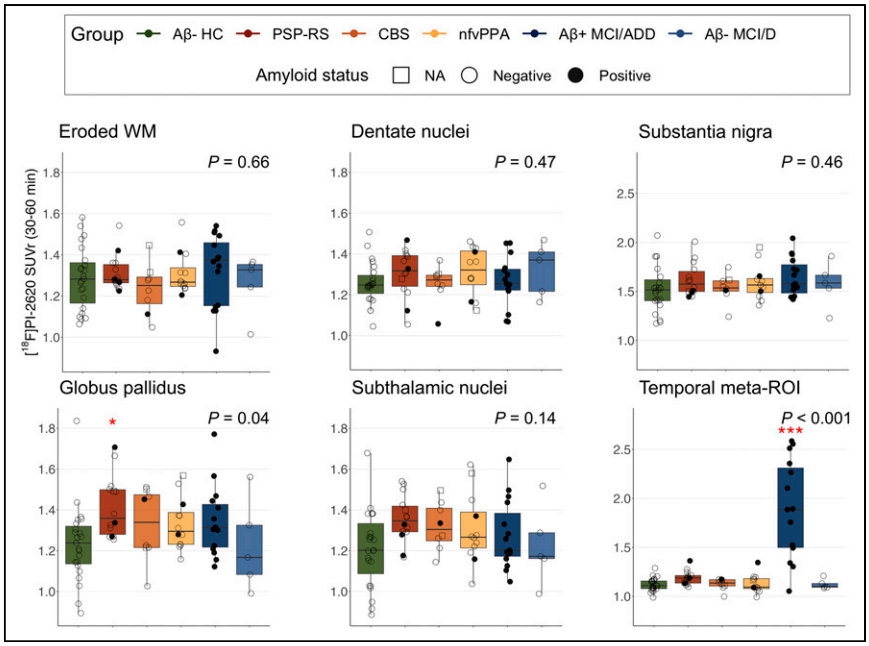

FIGURE 4. Mean [^{18}F]PI-2620 SUVr in selected regions compared among diagnostic groups. *P* corresponds to significance of group factor in analysis-of-covariance model comparing groups while controlling for age and sex. Three CBS AD patients are excluded from these plots (version with CBS AD is in Supplemental Fig. 11). Red stars indicate significance of difference compared with HC. *$P < 0.05$. ***$P < 0.001$. D = dementia; NA = not applicable; nfv = nonfluent variant; RS = Richardson syndrome.

temporoparietal, posterior, and frontal cortices in accordance with previous studies using [^{18}F]PI-2620 (*8,37*) or other tau PET radiotracers (*38,39*). Younger Aβ-positive MCI/ADD patients tended to have higher cortical binding than older ones, and the regional distribution of tracer varied with clinical variant (e.g., pronounced asymmetry in logopenic-variant PPA cases), similarly to previous [^{18}F]flortaucipir (*40,41*) and pathology studies (*42*). In the whole cohort, temporoparietal cortical binding was strongly associated with Aβ load and was elevated exclusively in patients with clearly positive Aβ PET scans (Figs. 1 and 5). Within the Aβ-positive MCI/ADD group, temporal [^{18}F]PI-2620 binding was associated with global cognitive function, as measured by the Mini-Mental State Examination. Besides the Aβ-positive MCI/ADD group, [^{18}F]PI-2620 PET suggested the presence of underlying AD neuropathology in several people with syndromes that are sometimes associated with AD, namely CBS and semantic-variant PPA. However, it is impossible to determine whether AD was the primary neuropathology in these cases or whether it cooccurred with another (e.g., FTLD) neuropathology. Similar to other tau PET tracers (*22*), [^{18}F]PI-2620 SUVr in the temporoparietal cortex consistently increased over time, and even though SUVr continued to elevate between 30 and 60 min after injection, discrimination between the Aβ-positive MCI/ADD and HC groups did not improve in later frames and was already high at 30–40 min after injection.

Patients with suspected FTLD had moderate binding in the basal ganglia, following the known neuropathologic distribution of tau aggregates in PSP and corticobasal degeneration (*43,44*). In particular, the PSP Richardson syndrome group had elevated pallidal binding, with a moderate frequency of abnormal binding at the individual level compared with the control group. The heterogeneity of pallidal SUVr in this group was at least partially related to disease severity as evidenced by its correlation to the PSP rating scale scores. This association contrasted with previously published results (*9*), which could be related to differences in the number of PSP Richardson syndrome patients and the tau PET quantification method (distribution volume ratio [DVR] vs. SUVr in this study). The association between tau uptake and PSP severity has been a matter of controversy for [^{18}F]flortaucipir PET too: some studies have found a positive correlation to SUVr in the globus pallidus (*45*) and midbrain (*46*), whereas others observed no association (*47,48*). Despite a variable disease duration in PSP Richardson syndrome and CBS patients, we did not observe binding in cortical regions that accumulate tau in later stages of these diseases, such as the frontoparietal, temporal, and motor cortices (*44,49*). Previous studies evaluated patients with PSP Richardson syndrome and CBS, but not nonfluent-variant PPA, which is also associated with underlying FTLD tau (PSP or more often corticobasal degeneration) in most cases (*20,50*). In the group analysis, nonfluent-variant PPA patients showed no significantly elevated binding compared with controls. Only 3 of 12 nonfluent-variant PPA patients (one of which was also Aβ-positive on PET) had an increased SUVr in the globus pallidus.

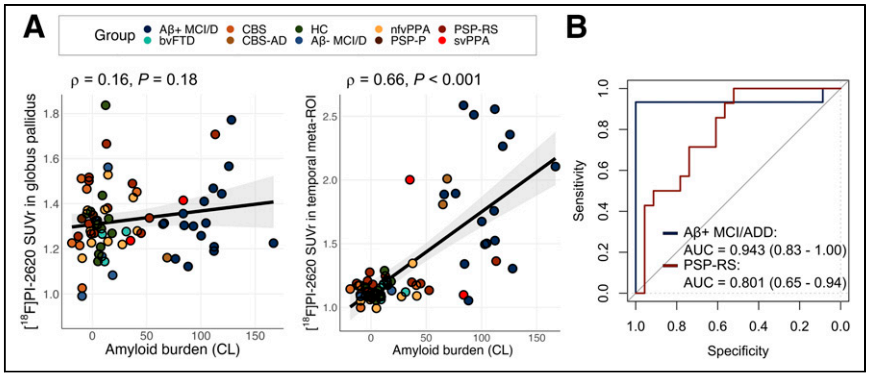

FIGURE 5. Associations between [^{18}F]PI-2620 SUVr in selected regions with Aβ burden (A) and respective AUC (B). In B, classification of Aβ-positive MCI/ADD group was based on SUVr in temporal meta-ROI whereas classification of PSP Richardson syndrome was based on SUVr in globus pallidus. bv = behavioral variant; CL = centiloid units; D = dementia; nfv = nonfluent variant; RS = Richardson syndrome; sv = semantic variant.

Considering the variability in types of filament structures across tauopathies, even within 4R tauopathies (*51*), [^{18}F]PI-2620 binding properties may vary depending on the type of tau lesion. Similarly to Kroth et al. (*6*), a recent study by Malarte et al. (*7*) demonstrated that the binding properties in corticobasal degeneration and PSP

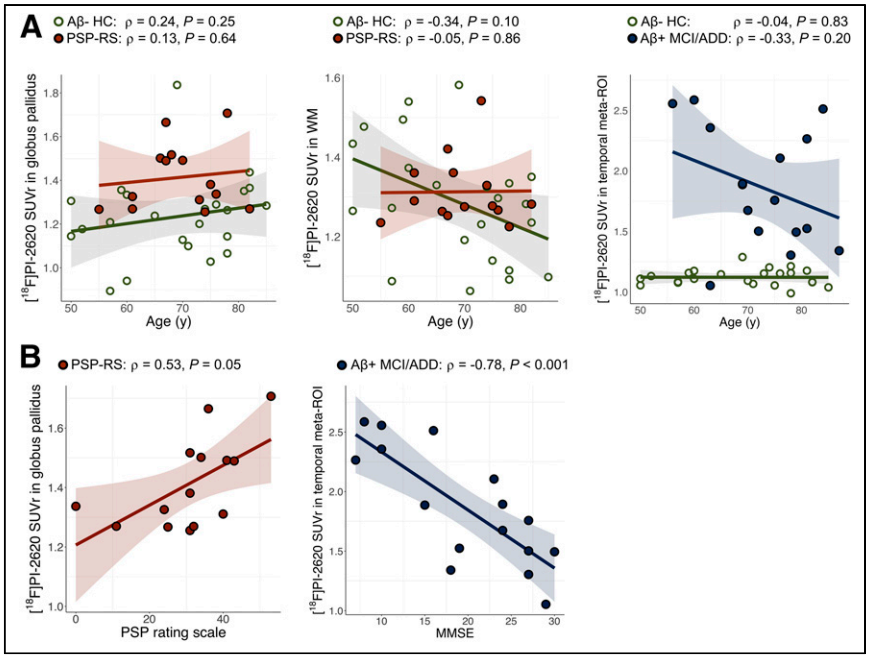

FIGURE 6. Results of correlation analyses between [^{18}F]PI-2620 binding (30–60 min) in selected regions and age (A) or disease severity (B). MMSE = Mini-Mental State Examination.

(dissociation constants, 1.2 and 0.2 nM, respectively) were almost comparable to those in AD (0.7 nM). Yet, there was a substantial difference in site density (maximum binding site density), suggesting up to almost a 6-fold difference between AD (3R/4R tau) and PSP (4R tau) (maximum binding site density, 69 and 12 fmol/mg, respectively) and almost a 3-fold difference between 4R tauopathies themselves (maximum binding site density, 32 and 12 fmol/mg for corticobasal degeneration and PSP, respectively). These differences can serve as a plausible explanation for why the [^{18}F]PI-2620 PET signal in patients with PSP was different from that in patients with CBS or nonfluent-variant PPA in our study and why binding levels of [^{18}F]PI-2620 were overall much lower in suspected FTLD than in AD tauopathies.

A high WM SUVr was present in multiple HC and FTLD participants, but there were no significant intergroup differences. We found no demographic (sex or race) or acquisition (scanner, site, or injected dose) characteristics that could explain the high WM binding. When present, WM retention was global and did not cluster in specific WM areas that would be expected from neuropathology findings (*52*) and previous [^{18}F]flortaucipir studies on FTLD, particularly in corticobasal degeneration (*47,53–56*). Some PSP Richardson syndrome and CBS patients had an elevated WM signal, but given the degree of WM binding in controls, this signal was considered nonspecific and cannot be used to differentiate these patients from HCs. High heterogeneity of WM SUVr in HCs and a tendency toward an age-related increase in binding are very similar to the variability of off-target binding in healthy aging reported for [^{18}F]flortaucipir (*57*). However, in contrast to [^{18}F]flortaucipir, we observed no relevant dentate binding for any FTLD subgroups.

Off-target [^{18}F]PI-2620 signal in the ventral midbrain and extracerebral areas was consistently present in all participants (*2,58*). Choroid plexus off-target binding was less consistently present than other types of off-target binding, in contrast to [^{18}F]flortaucipir or [^{18}F]PM-PBB3 tau PET (*59*). We observed no elevated choroid plexus binding at a group level, whereas a choroid plexus signal was clearly present in some patients and controls. In some participants, we also observed tracer binding in the meninges and pituitary gland (Supplemental Fig. 13). Moreover, in one participant with known meningioma, there was high tracer binding to the lesion (Supplemental Fig. 14). Within the brain parenchyma, "background" [^{18}F]PI-2620 off-target signal was relatively low but not absent: it varied in both patients and controls and increased with age in some regions, especially in the putamen, as indicated by regression analysis in HCs. First-generation tau PET tracers such as [^{18}F]flortaucipir are also limited by pronounced off-target binding in patients with non–tau-associated neurodegenerative disorders such as semantic-variant PPA (strongly predictive of FTLD TDP-43) or TDP-43–associated frontotemporal dementia. We found no elevated cortical [^{18}F]PI-2620 signal in the behavioral-variant frontotemporal dementia patients, including the *GRN* mutation carrier with significant cortical atrophy. However, the *GRN* mutation carrier showed elevated basal ganglia uptake. This finding is similar to the autopsy series report from our group published earlier demonstrating high [^{18}F]flortaucipir uptake in the basal ganglia of the *GRN* mutation carrier, but there was no tau pathology in this region (*60*). The semantic-variant PPA patient with a non-AD binding pattern showed a location and level of temporal binding similar to that of other Aβ-negative semantic-variant PPA patients previously scanned with [^{18}F]flortaucipir (*61,62*).

Evaluation of tracer binding in truncated acquisition windows indicated rapid washout of [^{18}F]PI-2620 from most target regions and WM at 30 min after injection. The absence of a significant interaction between group and time window indicated stable SUVr differences between groups for the selected time intervals. This effect was reflected in the receiver operating characteristic AUC analysis: the accuracy of classification between Aβ-positive MCI/ADD patients and HCs did not fluctuate much over time. In contrast, for PSP Richardson syndrome, CBS, and nonfluent-variant PPA, later time windows showed a better classification performance, but the difference in AUC was not significant (all $P > 0.1$, Supplemental Fig. 10C). This finding contradicts previous suggestions to use 20–40 min as an optimal static acquisition window for imaging FTLD (*11*). Moreover, the AUC for differentiating PSP Richardson syndrome patients from HCs was considerably lower than found by Song et al. (*11*) (0.77 vs. 0.94, respectively), even though the imaging windows overlapped substantially (30–60 vs. 20–40 min).

Simpler acquisition protocols, together with evaluation of parametric SUVr images with a common reference region, provide a highly relevant practical advantage over a 60-min dynamic acquisition with subsequent multilinear reference tissue modeling. Moreover, routine clinical practice demands shorter acquisition protocols; therefore, we have tested the feasibility of a 10-min static acquisition for AD and suspected FTLD classifications. SUVr from a 10-min static scan evaluation allowed for group separation, with an AUC of at least 0.94 and 0.77 for distinguishing Aβ-positive MCI/ADD and PSP Richardson syndrome patients, respectively, from HCs.

SUVr is convenient but might not be the best approach for evaluating [^{18}F]PI-2620 binding, as the underlying processes measured by the tracer in the 30- to 60-min time window are not at steady state.

This study had several limitations. First, part of the HC group stemmed from a previously published cohort (*9*). Both 4RTNI-2 and the University of California, San Francisco, Alzheimer's Disease Research Center studies enrolled HC participants; however, the number of controls enrolled at the time of analysis needed to be enriched with an external cohort. Second, the overall sample was relatively small, especially for some subgroups, such as PSP parkinsonism, CBS AD, semantic-variant PPA, or behavioral-variant frontotemporal dementia, which had to be dropped from further statistical analysis because of this consideration. This cohort also lacked participants with predicted FTLD due to TDP-43, which is the most likely underlying pathology in some clinical (e.g., semantic-variant PPA) and genetic (*C9orf72* mutation) syndromes on the FTLD spectrum. These participants might serve as a negative control group and supply missing information on [^{18}F]PI-2620 off-target binding and specificity to 4R tau. Third, all patients were diagnosed using current clinical criteria with no direct validation of the underlying pathology. Furthermore, our cohort was composed primarily of non-Hispanic, White individuals, limiting the generalizability of our results to other ethnocultural groups more representative of the diversity of individuals with AD and related dementias. Finally, application of abbreviated imaging protocols rather than a dynamic imaging protocol over 60 min, and analysis of SUVr instead of DVR, might have limited the ability to detect [^{18}F]PI-2620 binding in participants with suspected FTLD, although comparability of abbreviated/static and dynamic protocols has been shown for this tracer in other studies (*11*).

CONCLUSION

This multicenter study evaluating patients with suspected FTLD pathology suggested that a [^{18}F]PI-2620 PET 30- to 60-min SUVr has limited sensitivity for FTLD tau: elevated tracer retention was observed only in some clinical syndromes with FTLD, and there were varying levels of tracer binding at the single-subject level, even in PSP Richardson syndrome, where it performed best. Some level of binding in participants with suspected FTLD TDP pathology undermines the specificity of [^{18}F]PI-2620 and raises the question of whether a low-level signal here is related to tau burden or other processes that colocalize with tau. Autopsy validation and longitudinal evaluation are required to appraise whether [^{18}F]PI-2620 PET can potentially be used as a biomarker of FTLD tau. Therefore, use of [^{18}F]PI-2620 PET outside the AD spectrum should be interpreted with caution.

DISCLOSURE

Ganna Blazhenets was funded by the Deutsche Forschungsgemeinschaft (DFG, German Research Foundation)–493328842. David Soleimani-Meigooni received financial support from NIH/NIA K23-AG076960. Lawren VandeVrede receives financial support from NIA K23AG073514, has consulted for Retrope, and is the site principal investigator for clinical trials sponsored by Biogen. Julio Rojas is a site principal investigator for clinical trials sponsored by Eli Lilly and Eisai and receives support from NIH/NIA K23-AG059888. Bruce Miller received financial support from NIH/NIA P01-AG019724. Irene Litvan received research support from NIH 2R01AG038791-06A, U01NS100610, U01NS80818, R25NS098999, U19 AG063911-1, and 1R21NS114764-01A1; the Michael J. Fox Foundation, the Parkinson Foundation, the Lewy Body Association, CurePSP, Roche, Abbvie, Biogen, Centogene, EIP-Pharma, Biohaven Pharmaceuticals, Novartis, and United Biopharma SRL, UCB. She is a member of the scientific advisory board for the Rossy PSP Program at the University of Toronto and of the scientific advisory board for Amydis but does not receive funds. She is chief editor of *Frontiers in Neurology*. Alexander Pantelyat receives financial support from NIH/NIA K23-AG059891, NIH/NINDS U01-NS102035, and NIH/NIA R44-AG080861 and is on the scientific advisory board of MedRhythms, Inc. Adam Boxer received financial support from NIH/NIA R01-AG038791, U19-AG063911, Regeneron, Eisai, and Biogen and has received research support from Rainwater Charitable Foundation. He has served as a paid consultant for AGTC, Alector, Amylyx, Aviado-Bio, Arkuda, Arrowhead, Arvinas, Eli Lilly, Genentech, LifeEdit, Merck, Modalis, Oligomerix, Oscotec, Transposon, and Wave. Gil Rabinovici receives research support from NIH (P30-AG062422), the Alzheimer's Association, the American College of Radiology, Rainwater Charitable Foundation, Avid Radiopharmaceuticals, GE Healthcare, Genentech, and Life Molecular Imaging and has received consulting fees or speaking honoraria from Alector, Eli Lilly, GE Healthcare, Johnson & Johnson, Roche, Genentech, and Merck. He is an associate editor of *JAMA Neurology*. Life Molecular Imaging allowed use of [^{18}F]PI-2620. No other potential conflict of interest relevant to this article was reported.

ACKNOWLEDGMENTS

We thank the patients and their families.

KEY POINTS

QUESTION: Does a [^{18}F]PI-2620 tau PET 30- to 60-min SUVr allow diagnosis of patients with suspected AD and FTLD?

PERTINENT FINDINGS: Using the SUVr acquired at 30–60 min after injection, we observed high-intensity temporoparietal cortex–predominant [^{18}F]PI-2620 binding in patients with suspected AD, and this binding was significantly different from that in HCs. Patients with suspected FTLD exhibited lower-intensity pallidal binding that was higher than in controls but was heterogeneous and rapidly decreasing.

IMPLICATIONS FOR PATIENT CARE: [^{18}F]PI-2620 using a 30- to 60-min SUVr shows consistent binding in patients with suspected AD but varying levels of tracer binding in patients with suspected FTLD. The use of [^{18}F]PI-2620 PET outside the AD spectrum should be interpreted with caution.

REFERENCES

1. Ossenkoppele R, Rabinovici GD, Smith R, et al. Discriminative accuracy of [^{18}F]flortaucipir positron emission tomography for Alzheimer disease vs other neurodegenerative disorders. *JAMA.* 2018;320:1151–1162.
2. Mormino EC, Toueg TN, Azevedo C, et al. Tau PET imaging with ^{18}F-PI-2620 in aging and neurodegenerative diseases. *Eur J Nucl Med Mol Imaging.* 2021;48:2233–2244.
3. Irwin DJ, Cairns NJ, Grossman M, et al. Frontotemporal lobar degeneration: defining phenotypic diversity through personalized medicine. *Acta Neuropathol (Berl).* 2015;129:469–491.
4. Mackenzie IRA, Neumann M, Bigio EH, et al. Nomenclature and nosology for neuropathologic subtypes of frontotemporal lobar degeneration: an update. *Acta Neuropathol (Berl).* 2010;119:1–4.

5. Cairns NJ, Bigio EH, Mackenzie IRA, et al. Neuropathologic diagnostic and nosologic criteria for frontotemporal lobar degeneration: consensus of the Consortium for Frontotemporal Lobar Degeneration. *Acta Neuropathol (Berl).* 2007;114:5–22.
6. Kroth H, Oden F, Molette J, et al. Discovery and preclinical characterization of [^{18}F]PI-2620, a next-generation tau PET tracer for the assessment of tau pathology in Alzheimer's disease and other tauopathies. *Eur J Nucl Med Mol Imaging.* 2019; 46:2178–2189.
7. Malarte M-L, Gillberg P-G, Kumar A, Bogdanovic N, Lemoine L, Nordberg A. Discriminative binding of tau PET tracers PI2620, MK6240 and RO948 in Alzheimer's disease, corticobasal degeneration and progressive supranuclear palsy brains. *Mol Psychiatry.* 2023;28:1272–1283.
8. Bullich S, Mueller A, De Santi S, et al. Evaluation of tau deposition using ^{18}F-PI-2620 PET in MCI and early AD subjects: a MissionAD tau sub-study. *Alzheimers Res Ther.* 2022;14:105.
9. Brendel M, Barthel H, van Eimeren T, et al. Assessment of ^{18}F-PI-2620 as a biomarker in progressive supranuclear palsy. *JAMA Neurol.* 2020;77:1408–1419.
10. Palleis C, Brendel M, Finze A, et al. Cortical [^{18}F]PI-2620 binding differentiates corticobasal syndrome subtypes. *Mov Disord.* 2021;36:2104–2115.
11. Song M, Scheifele M, Barthel H, et al. Feasibility of short imaging protocols for [^{18}F]PI-2620 tau-PET in progressive supranuclear palsy. *Eur J Nucl Med Mol Imaging.* 2021;48:3872–3885.
12. Golbe LI, Ohman-Strickland PA. A clinical rating scale for progressive supranuclear palsy. *Brain.* 2007;130:1552–1565.
13. Hughes CP, Berg L, Danziger WL, Coben LA, Martin RL. A new clinical scale for the staging of dementia. *Br J Psychiatry.* 1982;140:566–572.
14. Miyagawa T, Brushaber D, Syrjanen J, et al. Utility of the global CDR® plus NACC FTLD rating and development of scoring rules: data from the ARTFL/LEFFTDS Consortium. *Alzheimers Dement.* 2020;16:106–117.
15. McKhann GM, Knopman DS, Chertkow H, et al. The diagnosis of dementia due to Alzheimer's disease: recommendations from the National Institute on Aging-Alzheimer's Association workgroups on diagnostic guidelines for Alzheimer's disease. *Alzheimers Dement.* 2011;7:263–269.
16. Gorno-Tempini ML, Hillis AE, Weintraub S, et al. Classification of primary progressive aphasia and its variants. *Neurology.* 2011;76:1006–1014.
17. Crutch SJ, Schott JM, Rabinovici GD, et al. Consensus classification of posterior cortical atrophy. *Alzheimers Dement.* 2017;13:870–884.
18. Höglinger GU, Respondek G, Stamelou M, et al. Clinical diagnosis of progressive supranuclear palsy: the Movement Disorder Society criteria. *Mov Disord.* 2017;32: 853–864.
19. Armstrong MJ, Litvan I, Lang AE, et al. Criteria for the diagnosis of corticobasal degeneration. *Neurology.* 2013;80:496–503.
20. Spinelli EG, Mandelli ML, Miller ZA, et al. Typical and atypical pathology in primary progressive aphasia variants. *Ann Neurol.* 2017;81:430–443.
21. Rascovsky K, Hodges JR, Knopman D, et al. Sensitivity of revised diagnostic criteria for the behavioural variant of frontotemporal dementia. *Brain.* 2011;134:2456–2477.
22. Baker SL, Lockhart SN, Price JC, et al. Reference tissue-based kinetic evaluation of ^{18}F-AV-1451 for tau imaging. *J Nucl Med.* 2017;58:332–338.
23. Sanchez JS, Hanseeuw B, Lopera F, et al. Longitudinal amyloid and tau accumulation in autosomal dominant Alzheimer's disease: findings from the Colombia-Boston (COLBOS) biomarker study. *Alzheimers Res Ther.* 2021;13:27.
24. Gordon BA, Blazey TM, Christensen J, et al. Tau PET in autosomal dominant Alzheimer's disease: relationship with cognition, dementia and other biomarkers. *Brain.* 2019;142:1063–1076.
25. Arboleda-Velasquez JF, Lopera F, O'Hare M, et al. Resistance to autosomal dominant Alzheimer's disease in an APOE3 Christchurch homozygote: a case report. *Nat Med.* 2019;25:1680–1683.
26. Lopera F, Marino C, Chandrahas AS, et al. Resilience to autosomal dominant Alzheimer's disease in a Reelin-COLBOS heterozygous man. *Nat Med.* 2023;29:1243–1252.
27. Diedrichsen J, Maderwald S, Küper M, et al. Imaging the deep cerebellar nuclei: a probabilistic atlas and normalization procedure. *Neuroimage.* 2011;54:1786–1794.
28. Klunk WE, Koeppe RA, Price JC, et al. The Centiloid Project: standardizing quantitative amyloid plaque estimation by PET. *Alzheimers Dement.* 2015;11:1–15.e1–4.
29. Royse SK, Minhas DS, Lopresti BJ, et al. Validation of amyloid PET positivity thresholds in centiloids: a multisite PET study approach. *Alzheimers Res Ther.* 2021;13:99.
30. La Joie R, Bejanin A, Fagan AM, et al. Associations between [^{18}F]AV1451 tau PET and CSF measures of tau pathology in a clinical sample. *Neurology.* 2018;90: e282–e290.
31. Roemer SF, Grinberg LT, Crary JF, et al. Rainwater Charitable Foundation criteria for the neuropathologic diagnosis of progressive supranuclear palsy. *Acta Neuropathol (Berl).* 2022;144:603–614.
32. Jack CR, Wiste HJ, Weigand SD, et al. Defining imaging biomarker cut points for brain aging and Alzheimer's disease. *Alzheimers Dement.* 2017;13:205–216.
33. Ilinsky I, Horn A, Paul-Gilloteaux P, Gressens P, Verney C, Kultas-Ilinsky K. Human motor thalamus reconstructed in 3D from continuous sagittal sections with identified subcortical afferent territories. *eNeuro.* 2018;5:ENEURO.0060-18.2018.
34. Carpenter J, Bithell J. Bootstrap confidence intervals: when, which, what? A practical guide for medical statisticians. *Stat Med.* 2000;19:1141–1164.
35. Koga S, Josephs KA, Aiba I, Yoshida M, Dickson DW. Neuropathology and emerging biomarkers in corticobasal syndrome. *J Neurol Neurosurg Psychiatry.* 2022;93:919–929.
36. La Joie R, Ayakta N, Seeley WW, et al. Multisite study of the relationships between antemortem [^{11}C]PIB-PET centiloid values and postmortem measures of Alzheimer's disease neuropathology. *Alzheimers Dement.* 2019;15:205–216.
37. Mueller A, Bullich S, Barret O, et al. Tau PET imaging with ^{18}F-PI-2620 in patients with Alzheimer disease and healthy controls: a first-in-humans study. *J Nucl Med.* 2020;61:911–919.
38. Leuzy A, Smith R, Ossenkoppele R, et al. Diagnostic performance of RO948 F 18 tau positron emission tomography in the differentiation of Alzheimer disease from other neurodegenerative disorders. *JAMA Neurol.* 2020;77:955–965.
39. Pascoal TA, Therriault J, Benedet AL, et al. ^{18}F-MK-6240 PET for early and late detection of neurofibrillary tangles. *Brain.* 2020;143:2818–2830.
40. La Joie R, Visani AV, Lesman-Segev OH, et al. Association of APOE4 and clinical variability in Alzheimer disease with the pattern of tau- and amyloid-PET. *Neurology.* 2021;96:e650–e661.
41. Whitwell JL, Graff-Radford J, Tosakulwong N, et al. Imaging correlations of tau, amyloid, metabolism, and atrophy in typical and atypical Alzheimer's disease. *Alzheimers Dement.* 2018;14:1005–1014.
42. Petersen C, Nolan AL, de Paula França Resende E, et al. Alzheimer's disease clinical variants show distinct regional patterns of neurofibrillary tangle accumulation. *Acta Neuropathol (Berl).* 2019;138:597–612.
43. Dickson DW, Kouri N, Murray ME, Josephs KA. Neuropathology of frontotemporal lobar degeneration–tau (FTLD-tau). *J Mol Neurosci.* 2011;45:384–389.
44. Kovacs GG, Lukic MJ, Irwin DJ, et al. Distribution patterns of tau pathology in progressive supranuclear palsy. *Acta Neuropathol (Berl).* 2020;140:99–119.
45. Smith R, Schain M, Nilsson C, et al. Increased basal ganglia binding of ^{18}F-AV-1451 in patients with progressive supranuclear palsy. *Mov Disord.* 2017;32:108–114.
46. Whitwell JL, Lowe VJ, Tosakulwong N, et al. [^{18}F]AV-1451 tau-PET in progressive supranuclear palsy. *Mov Disord.* 2017;32:124–133.
47. Schonhaut DR, McMillan CT, Spina S, et al. ^{18}F-flortaucipir tau positron emission tomography distinguishes established progressive supranuclear palsy from controls and Parkinson disease: a multicenter study. *Ann Neurol.* 2017;82:622–634.
48. Cho H, Choi JY, Hwang MS, et al. Subcortical ^{18}F-AV-1451 binding patterns in progressive supranuclear palsy. *Mov Disord.* 2017;32:134–140.
49. Forrest SL, Kril JJ, Halliday GM. Cellular and regional vulnerability in frontotemporal tauopathies. *Acta Neuropathol (Berl).* 2019;138:705–727.
50. Villemagne VL, Fodero-Tavoletti MT, Masters CL, Rowe CC. Tau imaging: early progress and future directions. *Lancet Neurol.* 2015;14:114–124.
51. Scheres SH, Zhang W, Falcon B, Goedert M. Cryo-EM structures of tau filaments. *Curr Opin Struct Biol.* 2020;64:17–25.
52. Coughlin DG, Hiniker A, Peterson C, et al. Digital histological study of neocortical grey and white matter tau burden across tauopathies. *J Neuropathol Exp Neurol.* 2022;81:953–964.
53. Tsai RM, Bejanin A, Lesman-Segev O, et al. ^{18}F-flortaucipir (AV-1451) tau PET in frontotemporal dementia syndromes. *Alzheimers Res Ther.* 2019;11:13.
54. Ali F, Whitwell JL, Martin PR, et al. [^{18}F] AV-1451 uptake in corticobasal syndrome: the influence of beta-amyloid and clinical presentation. *J Neurol.* 2018;265: 1079–1088.
55. Cho H, Baek MS, Choi JY, et al. ^{18}F-AV-1451 binds to motor-related subcortical gray and white matter in corticobasal syndrome. *Neurology.* 2017;89:1170–1178.
56. Smith R, Schöll M, Widner H, et al. In vivo retention of ^{18}F-AV-1451 in corticobasal syndrome. *Neurology.* 2017;89:845–853.
57. Baker SL, Harrison TM, Maass A, Joie RL, Jagust WJ. Effect of off-target binding on ^{18}F-flortaucipir variability in healthy controls across the life span. *J Nucl Med.* 2019;60:1444–1451.
58. Tezuka T, Takahata K, Seki M, et al. Evaluation of [^{18}F]PI-2620, a second-generation selective tau tracer, for assessing four-repeat tauopathies. *Brain Commun.* 2021;3:fcab190.
59. Tagai K, Ono M, Kubota M, et al. High-contrast in vivo imaging of tau pathologies in Alzheimer's and non-Alzheimer's disease tauopathies. *Neuron.* 2021;109:42–58.e8.
60. Soleimani-Meigooni DN, Iaccarino L, La Joie R, et al. ^{18}F-flortaucipir PET to autopsy comparisons in Alzheimer's disease and other neurodegenerative diseases. *Brain.* 2020;143:3477–3494.
61. Smith R, Santillo AF, Waldö ML, et al. ^{18}F-flortaucipir in TDP-43 associated frontotemporal dementia. *Sci Rep.* 2019;9:6082.
62. Pascual B, Funk Q, Zanotti-Fregonara P, et al. Neuroinflammation is highest in areas of disease progression in semantic dementia. *Brain.* 2021;144:1565–1575.